JOURNAL OF SOLID STATE CHEMISTRY 73, 191–199 (1988)

Study of the Nature of Extended Defects of Copper Oxide

G. N. KRYUKOVA, V. I. ZAIKOVSKII, V. A. SADYKOV,*
S. F. TIKHOV, V. V. POPOVSKII, AND N. N. BULGAKOV

Institute of Catalysis, Siberian Branch of the USSR Academy of Sciences,
Prospekt Lavrentieva, 5, Novosibirsk 630090, USSR

Received January 5, 1987; in revised form September 28, 1987

A sample of powdered copper oxide suitable for studying its real structure with the help of electron microscopy was prepared by slow decomposition of copper nitrate. It is shown that in particles of oxide there are (001) and (100) twins and screw dislocations with Burgers vector along ⟨010⟩. The lattice of CuO near the twins is strongly deformed. The structures of the composition planes for both types of twins as well as their relative stabilities are analyzed. © 1988 Academic Press, Inc.

Introduction

The synthesis of catalysts with desirable properties is intimately connected with the nature of surface active centers. In this connection it is very important to study the morphology and defect structure of catalyst particles with the aid of electron microscopy (EM) (*1, 2*).

We have shown previously (*3–5*) that one of the most widely used active components of the oxide catalysts—copper oxide—has a high catalytic activity in the oxidation by molecular oxygen, because of active centers associated with dislocations on the surface. Up to the present there is a lack of information concerning the characteristics of the extended defects in CuO. Moreover the samples of CuO investigated earlier were not suitable for the study by EM because of the thickness of those particles.

The aim of this work was to prepare a sample of CuO suitable for EM and to study the extended defects and their properties.

Experimental

For the synthesis of CuO, a 3.64 *M* solution of copper nitrate "pure for analysis" grade was slowly evaporated to dryness. The residue was placed in a crucible and calcined at 400°C for 4 hr in a muffle furnace.

According to X-ray analysis the sample obtained was pure tenorite (CuO); its specific surface determined by low temperature argon adsorption was 0.5 m^2/g.

The sample was examined in a JEM-100C electron microscope fitted with a tilt side entry goniometer stage and operated at 100 kV. The specimen was prepared by dispersion in ethanol and allowing a drop of suspension to dry on a holey carbon film supported on a copper grid.

Results

The crystal structure of CuO (tenorite) conforms to the space group $C2/c$ of the monoclinic system; the parameters of the unit cell (Fig. 1) are $a = 4.6834 \pm 5$ Å; $b =$

---

* To whom correspondence should be addressed.

0022-4596/88 $3.00

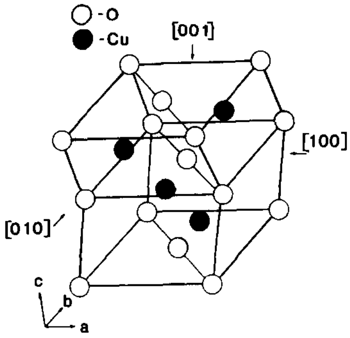

FIG. 1. The unit cell of tenorite.

3.4226 ± 5 Å; $c = 5.1288 \pm 6$ Å; $\beta = 99°54'$ (*6*).

The sample of copper oxide under investigation consisted of thin elongated platelets, not more than 500 Å thick and 10^3 Å wide. Figure 2 shows the most common platelet of CuO. The (010) face was the most highly developed one and usually was in the plane of projection. The lateral parts of the platelets were mainly (001) faces and (100) faces that were strongly jagged.

The predominant part of CuO crystals was polysynthetically twinned with (001) habit plane. In Fig. 3 these twins are seen as periodically recurring bands ~100–200 Å wide. The analysis of a selected area electron diffraction pattern revealed diffraction spots from twin blocks. Figures 4a and 4b show the diffraction pattern from the ⟨010⟩ orientation and a corresponding scheme. Pairs of spots 002 and 002_t, 202 and $\bar{2}02_t$, 402 and $\bar{4}02_t$, etc., are seen, where the t refers to the twinned portion. One may determine the twin angle using the relation $\sin \alpha_l/2 = a/6c$; $\alpha_l = 17°30'$. The linear concentration of twin interfaces may be as high as 10^6 cm^{-1}. On an enlarged image of the twin region (Fig. 5) it is seen that within each band there are variations of contrast caused by extinction contours which lack periodicity and are not straight. Such contours may be associated with microstrains of the lat-

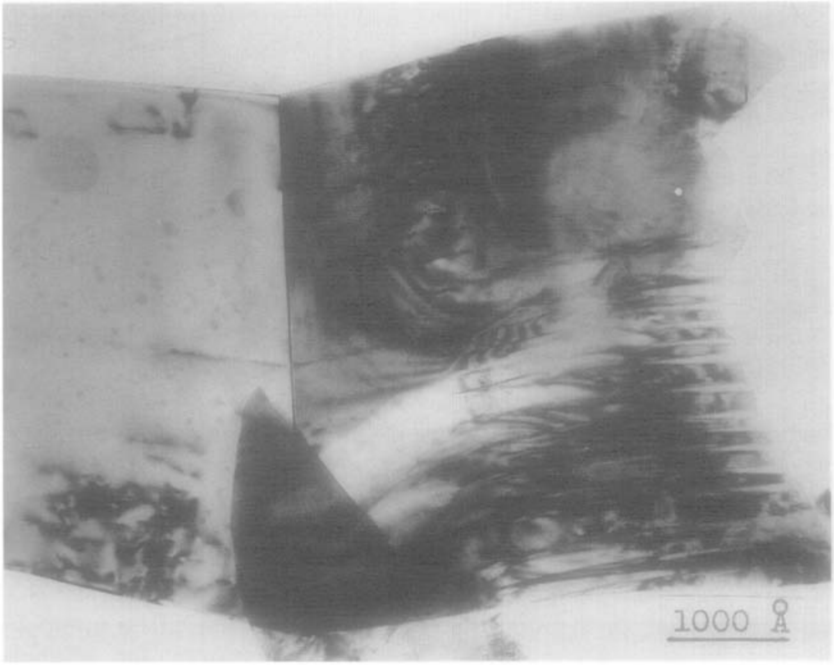

FIG. 2. Micrograph of the most common platelet of CuO.

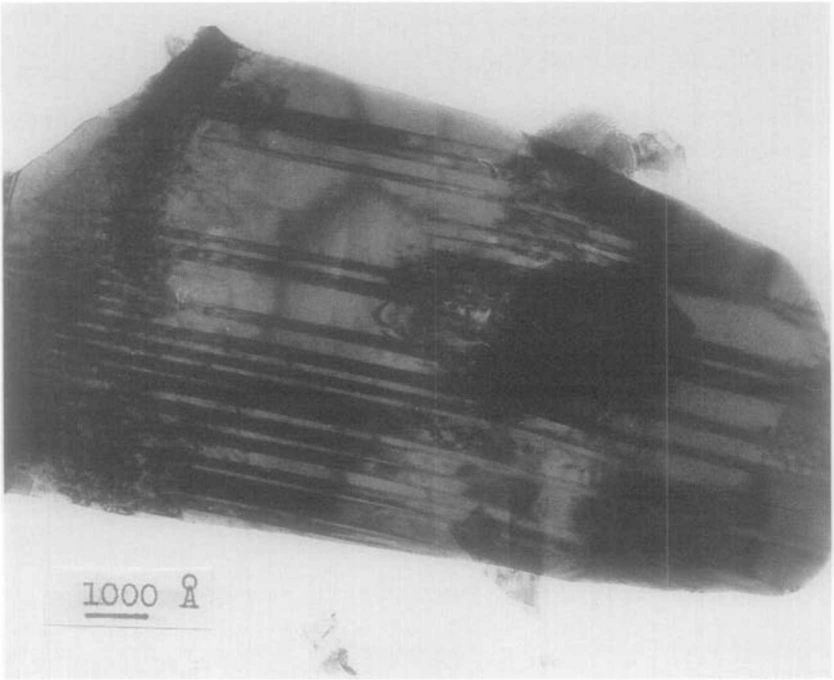

FIG. 3. Image of the platelet with polysynthetical (001) twinning.

tice (1). In proceeding from one twin block to another, the alteration of contrast derives from differences in their crystallographic orientation. The twin boundaries are seen as narrow lines if the electron beam is parallel to them or as periodic bands with small periods when the sample is slightly misaligned (7).

Twins with (100) twin boundary are not as common as (001). Usually on a CuO

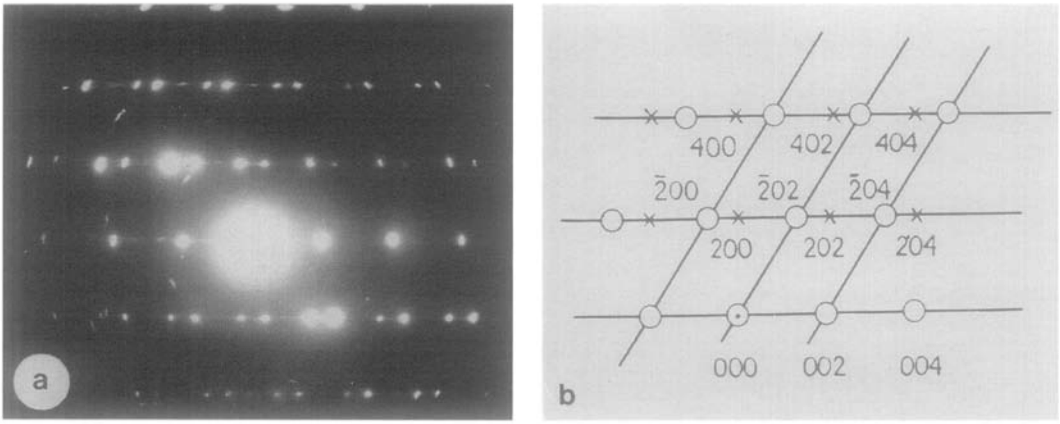

FIG. 4. Selected area electron diffraction pattern from the (001) twin region (a) and a corresponding scheme (b).

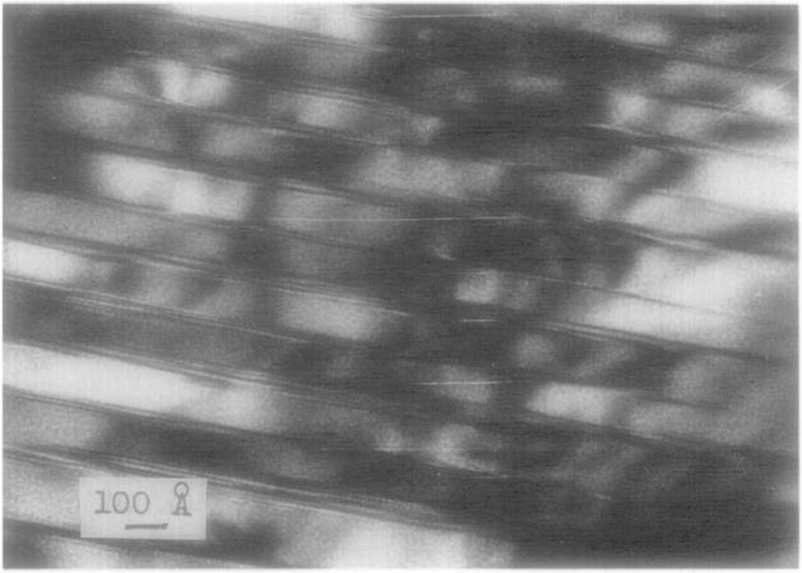

FIG. 5. Enlarged image of the (001) twin region.

platelet not more than one twin interface of this type can be detected as a narrow band with strong contrast (Fig. 1). Therefore, the density of these twins is less than 10^4 cm^{-1}. Diffraction pattern from the (100) twin and a corresponding scheme are shown in Figs. 6a and 6b. Consequently, for the twinning angle one may write: $\sin \alpha_2/2 = c/6a$; $\alpha_2 = 21°41'$.

Figure 1 shows that the pecularities of morphology of the crystals are due to the twins. Thus, polysynthetic twinning produces many steps on (100) faces, while (100) twinning is accompanied by intersection of (001) lateral faces at angles of ca. 20°.

Some crystals of CuO are characterized by the simultaneous appearance of both types of twins (Fig. 7). It is reasonable to expect a substantial disordering of these re-

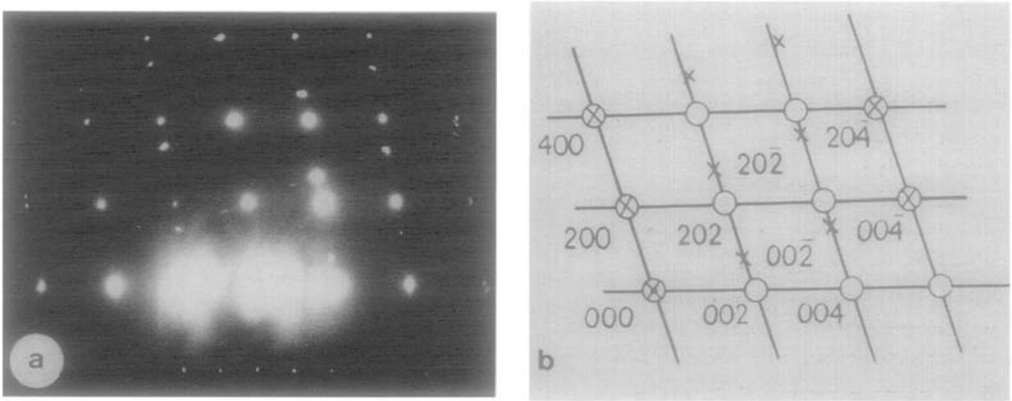

FIG. 6. Selected area electron diffraction pattern from the (100) twin region (a) and a corresponding scheme (b).

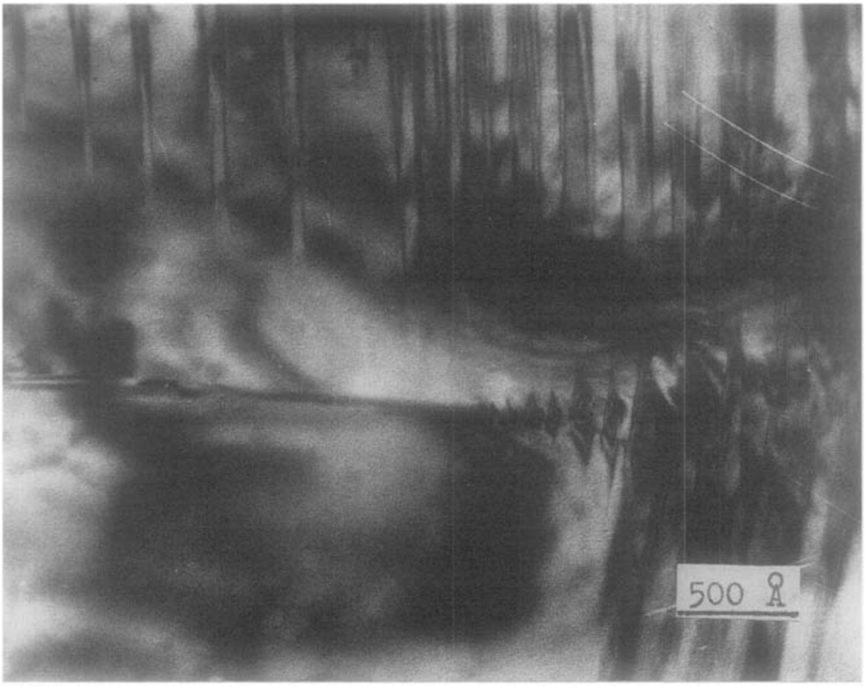

FIG. 7. Region of the intersection of both types of twins.

gions due to incoherent stacking of the twinned blocks.

In addition to twins a wide range of dislocation lines is seen in the micrographs of specimen. There is a lack of data concerning the dislocation structure for the CuO system with monoclinic symmetry. This seems to be connected with the very large computer calculations which are required for a full interpretation of the dislocation contrast. Nevertheless it is possible to draw conclusions about the type of dislocations observed by simple physical and structural means, as in (*2*). A detailed analysis of the dislocation contrast will be provided in a separate publication.

Figures 8a and 8b show typical bright and dark field images of the same area of CuO crystal, where **g** is the reciprocal lattice vector of the imaging reflection. Note the regions of strong contrast marked by the letter A. This contrast was visible in any reflection from the ⟨010⟩ zone as well as after the tilting of the specimen (the standard criterion $g \cdot b = 0$ was not realized). The bright field image demonstrates the periodic alteration of the contrast. The contrast in the dark field image has a "zigzag" character. Detailed computer calculation of the image contrast was made (*8*) for the inclined dislocation lying close to the specimen surface. In our case we have observed a similar variation of contrast. Therefore we may suppose that the strong contrast in region A is caused by an inclined dislocation which, on emerging in the (010) plane, has a step attached to it.

Another type of the complex contrast was observed in the vicinity of the twin boundaries (Fig. 8b, marked by the letter B). It may be due to the presence of twin dislocations (or steps) on the habit plane as in (*2*), but the imaging conditions are not sufficiently well defined to warrant further analysis here.

A third type of contrast is shown in Fig.

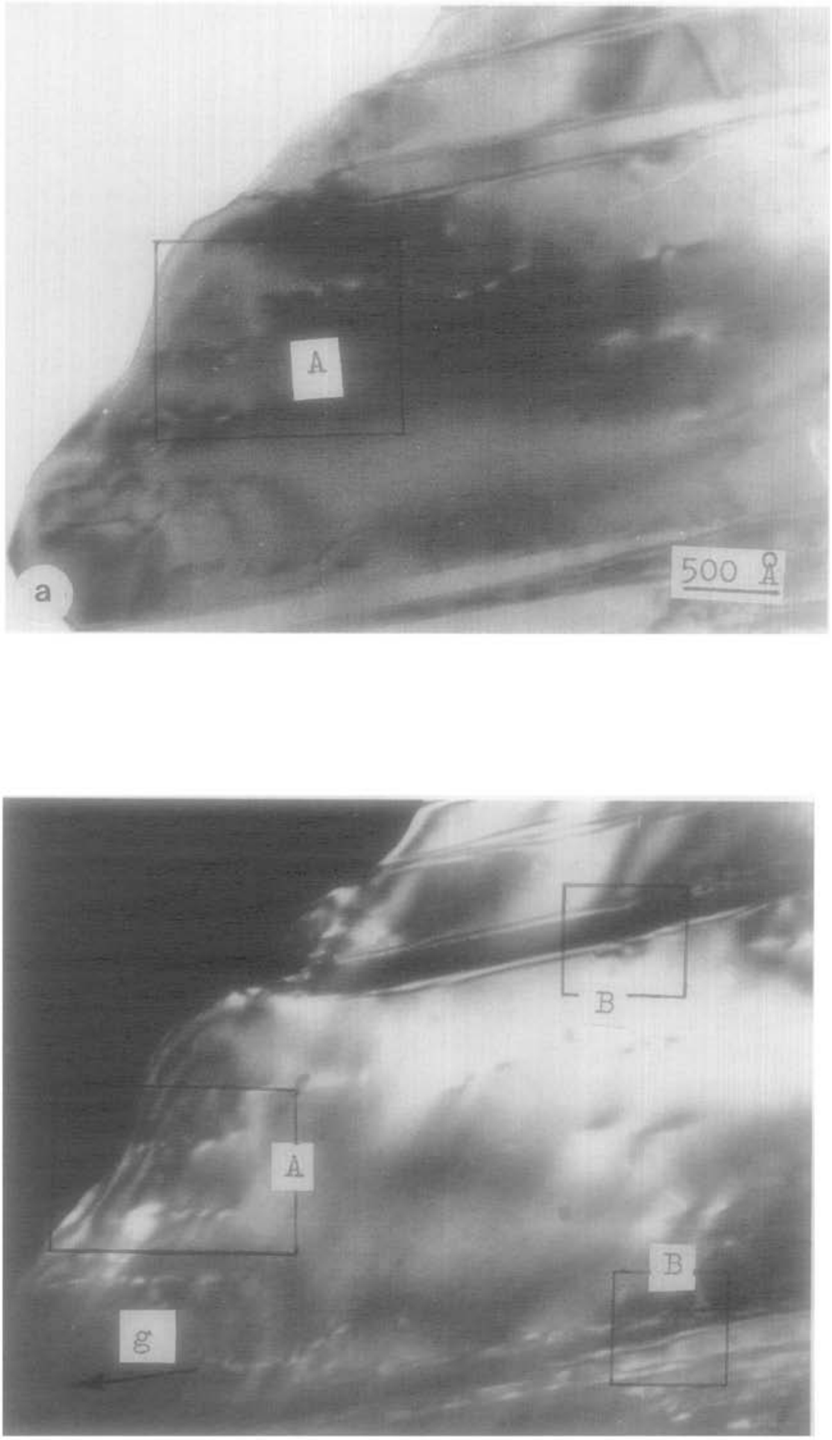

FIG. 8. Bright (a and c) and dark field (b) images of a CuO crystal oriented at the ⟨010⟩ zone. See text for further discussion.

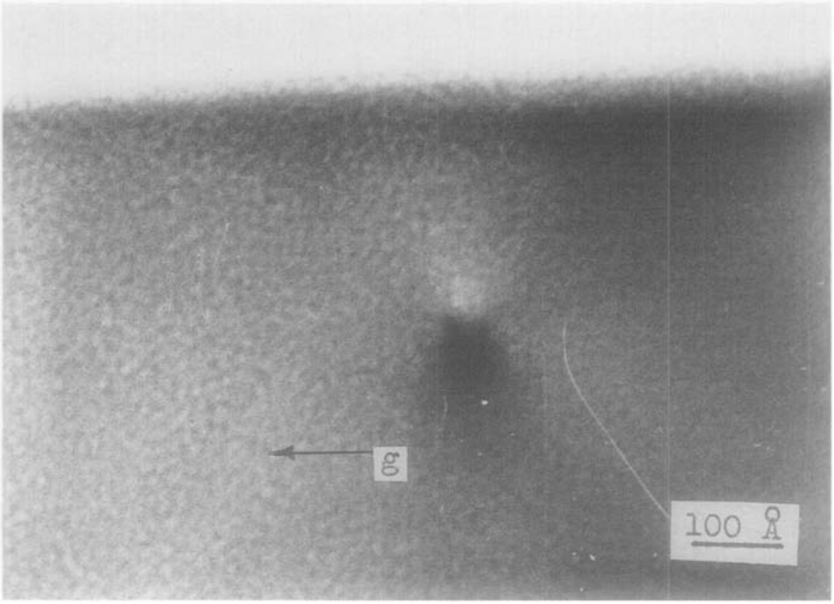

FIG. 8—*Continued.*

8c. The line dividing the bright and dark part of the image is parallel to **g**. Usually this type of contrast is associated with a dislocation normal to the specimen surface (*1*). In this case the contrast appears as a result of the surface displacements in the vicinity of outlets of dislocations.

Discussion

The determination of the detailed structure of the twin boundaries is based on the high-resolution electron microscopy images and its computer simulations. In the recent literature the direct imaging of the atomic positions was carried out for structures whose symmetry is no lower than tetragonal or orthorhombic. Nevertheless it seems useful by analogy with (*2*) to carry out a comparable analysis of the possible structures of the twin boundaries, choosing the most probable ones on the basis of thermodynamic calculations.

In general, twinning results either from a reflection in the twin plane or by a twisting of the twin axis and a subsequent translation. In our case we have examined the mirror twinning.

Consider the possible structures of the CuO crystal near the habit planes (Figs. 9a and 9b). In these regions the distance between copper atoms ($r_{\text{Cu-Cu}}$) is substantially less than $r_{\text{Cu-Cu}}$ for the ideal structure of CuO (2.88 Å). Estimates show that $r_{\text{Cu-Cu}}$ for a (001) twin is 2.52 Å; for a (100) twin it is 2.30 Å, which is less than $r_{\text{Cu-Cu}}$ in metallic copper. Such small distances may explain a considerable strain of the lattice in the vicinity of extended defects.

For the discrimination of the relative stability of various twinnings it is necessary to evaluate their excess free energy of formation or, more particularly, their excess enthalpy. For this purpose we have used the method of semiempirical quantum chemical interacting bonds (*9*). As may be seen from Figs. 9 and 9b in the vicinity of the habit planes oxygen ions are in the centers of planar squares, rather than of tetrahedra typical for ideal CuO (*6*). To estimate the heat

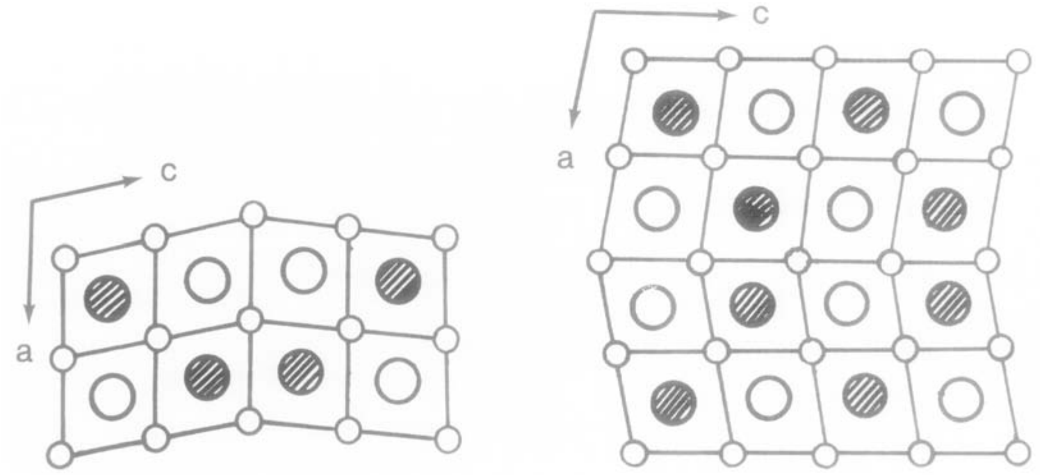

FIG. 9. A (010) projection of the twin region with different types of twinning; (a) (100), (b) (001). Large open circles correspond to Cu atoms at a height of 0.75 **b**; large filled circles = Cu atoms at a height of 0.25 **b**; small open circles = oxygen atoms.

of atomization of CuO in these regions we took into consideration the dependence of the interaction energy of Cu–O bonds on the angle between them, as in (*10*). According to the calculations the formation of mirror (001) twins should enhance the enthalpy of formation by ~9 kJ/mole CuO involved in this defect, while the formation of mirror (100) twins, by ~13 kJ/mole in comparison with the enthalpy of formation of ideal CuO. These values are in a good agreement with the frequency of the appearance of these defects and indicate their relative stability. The calculated values of twin energies (ca. 2×10^{-1} J/m^2) are quite close to the energies of twins and grain boundaries in copper (4×10^{-2} J/m^2 and 6×10^{-1} J/m^2 (*11*), respectively) as well as to the twin energies in spinel structures (3×10^{-2} J/m^2 (*12*)). Therefore, our method of calculation is substantially more accurate than that usually employed, based on consideration of electrostatic forces; these yield planar faults energies greater by ca. 2 order of magnitude than experimental values (*13–16*).

In the vicinity of the twin plane the anion sublattice is practically undisturbed; this may be the reason for the low energy of twin formation. Analysis has revealed that other types of twins (glide twins) inevitably result in higher energies of formation and therefore are less probable.

As is evident from the analysis of the defect structure of CuO the (001) plane is the most preferable for the formation of planar and linear defects. The surface defects in the form of monoatomic steps inevitably appear at outlets of dislocations. Therefore, we expect that the most developed (010) face of CuO crystals contains a great number of surface defects of this kind. Usually the coordination of atoms is changed at steps (*17*) and in twin planes (*18*) in comparison with atoms on flat surfaces. Since the coordination significantly influences the catalytic properties of oxides (*19*) we may suppose that at least a portion of the active centers is associated with outlets of extended defects on CuO surfaces. A verification of this supposition will be provided in the companion article.

References

1. P. B. Hirsch, A. Howie, R. B. Nickolson, D. W. Pashly, and M. J. Whelan, "Electron Microscopy of Thin Crystals," Butterworths, London (1965).
2. L. A. Bursill and R. L. Withers, *Philos. Mag. A* **40,** 213 (1979).
3. V. A. Sadykov, S. F. Tikhov, V. V. Popovskii, G. N. Kryukova, and L. A. Isupova, *Kinet. Katal.* **26,** 168 (1985).
4. Yu. A. Lokhov, V. A. Sadykov, S. F. Tikhov, and V. V. Popovskii, *Kinet. Katal.* **26,** 177 (1985).
5. V. A. Sadykov, S. F. Tikhov, and V. V. Popovskii, *Kinet. Katal.* **27,** 147 (1986).
6. S. Åsbrink and L.-J. Norrby, *Acta Crystallogr. Sect. B* **26,** 8 (1970).
7. J. D. Tilley and A. C. Wright, *J. Solid State Chem.* **65,** 42 (1986).
8. A. Howie and M. J. Whelan, *Proc. R. Soc. London Ser. A* **267,** 206 (1962).
9. N. N. Bulgakov, Yu. A. Borisov, and V. V. Popovskii, *Kinet. Katal.* **14,** 469 (1973).
10. O. N. Shumilo, N. N. Bulgakov, and V. A. Likholobov, *React. Kinet. Catal. Lett.* **22,** 87 (1983).
11. J. P. Hirth and J. Lothe, "Theory of Dislocations," McGraw–Hill, London (1968).
12. W. T. Donlon, T. E. Mitchell, and A. H. Heuer, *Philos. Mag. A* **40,** 351 (1979).
13. P. Veyssiére, J. Babier, H. Garem, and J. Grilhé, *Philos. Mag. A* **38,** 61 (1978).
14. P. Veyssiére, J. Babier, and J. Grilhé, *Phys. Status Solidi A* **34,** 605 (1975).
15. G. Fontaine, *J. Phys. Chem. Solids* **29,** 209 (1968).
16. B. S. Tiwari, A. K. Bai, and O. N. Srivastava, *Phys. Status Solidi A* **31,** 941 (1975).
17. G. A. Somorjai, *in* "Proceedings of the 8th International Congress on Catalysis," Vol. 1, p. 113, West Berlin (1984).
18. J. D. Tilley, *in* "Surface Properties and Catalysis by Non-Metals" (J. P. Bonnete, B. Demon, and E. Derouane, Eds.), Reidel, Dodrecht (1983).
19. G. K. Boreskov, *in* "Proceedings of the 6th International Congress on Catalysis," Vol. 1, p. 204, London (1976).